Journal of the Geological Society, London, Vol. **163**, 2006, pp. 143–148. Printed in Great Britain.

Active deformation within the Zagros Mountains deduced from GPS measurements

KHALED HESSAMI[1,2], FARAMARZ NILFOROUSHAN[1,3] & CHRISTOPHER J. TALBOT[1]

[1]*Hans Ramberg Tectonic Laboratory, Department of Earth Sciences, Uppsala University, SE-752 36 Uppsala, Sweden*

[2]*International Institute of Earthquake Engineering and Seismology, PO Box 19395/3913, Tehran, Iran (e-mail: hessami@iiees.ac.ir)*

[3]*Research Institute of National Cartographic Center (RINCC), PO Box 13185-1684, Tehran, Iran*

Abstract: We present and interpret the results of Global Positioning System (GPS) measurements at 35 stations in and beside the Zagros Mountain belt, SW Iran, for three campaigns ending March 1998, December 1999 and June 2001. Preliminary motion estimates show clearly the change in character along the strike of the belt. Stations to the SE move at 13–22 ± 3 mm a^{-1} towards N 7 ± 5°E with respect to Eurasia. Most of the shortening indicated by the GPS velocities seems to occur in the SE Zagros along two major seismic zones and along the Zagros front. To the NW, stations move oblique to the trend of the belt towards N 12 ± 8°W, at 14–19 ± 3 mm a^{-1}. Most of the shortening in the NW Zagros seems to occur along the Mountain Front Fault with its major earthquakes as well as along the Zagros front. The change in direction and magnitude of the velocity vectors across the north–south-trending Kazerun and Karebas faults involves extension of up to 4 mm a^{-1} along the strike of the Zagros belt.

Various workers have determined the rate and direction of convergence between Arabia and Eurasia across Iran (which includes the Zagros) by summing the rotational vectors of pertinent plate motions (Le Pichon 1968; McKenzie 1972). Their results show nearly north–south convergence at a rate of 43–48 mm a^{-1}. Using spreading rates, transform fault azimuths and earthquake slip vectors, DeMets *et al*. (1990) calculated a north–south convergence rate of about 31 mm a^{-1} at 30°N, 51.5°E. Jackson & McKenzie (1984) added movement vectors for central Iran relative to Eurasia to those of Arabia relative to Eurasia to locate the Arabia–central Iran pole of rotation near 34.5°N, 39.8°E. They estimated that the Arabian plate is moving NE relative to central Iran at a rate of 0.95° Ma^{-1}. This is equivalent to about 10 mm a^{-1} in the NW Zagros and 26 mm a^{-1} in the SE Zagros further from the pole of rotation.

The rate of active orogenic processes anywhere was first constrained in the SW Zagros region by Lees & Falcon (1952). They showed that a canal bed about 1700 years old was deepened 12 ft (4 m) to take account of the slow rise of the Shaur anticline. This can be interpreted to imply an anticlinal uplift rate of about 2.3 mm a^{-1}. Falcon (1974) then inferred that the regional uplift represented by 'geo-flexure' implied that the Zagros had risen at a minimum rate of 1 mm a^{-1} since the early Pliocene.

Some of the first ^{14}C dates were applied to uplifted marine terraces along the Persian Gulf coast and indicated that the flanks of frontal anticlines in the Zagros rose episodically at rates of 0.7 mm a^{-1} for about 7000 years (Vita-Finzi 1979, after the eustatic factor of Clark *et al*. is taken into account). This was interpreted to imply a long-term average rate of northeastward frontal shortening of about 6.8 mm a^{-1} (Vita-Finzi 1979), close to the cumulative average propagation rate of about 10 mm a^{-1} of the Zagros front since the Eocene (Hessami *et al*. 2001*a*).

Modern seismicity also shows active crustal shortening across the Zagros plate boundary (see Fig. 2). The shortening rate estimated from the seismic moments of earthquakes is only 1–2 mm a^{-1} (Shoja-Taheri & Niazi 1981; Jackson & McKenzie 1988), which is a minimum because aseismic deformation is not included in the calculations.

The present crustal shortening associated with the convergence between Arabia and Eurasia is clearly shown in recent Global Positioning System (GPS) results spanning Iran (Nilforoushan *et al*. 2003; Vernant *et al*. 2004). These velocity estimates show that Arabia moves at 21–25 mm a^{-1} north relative to Eurasia. However, deformation is distributed differently over several active deformation zones. Using a few stations located in the Zagros, Nilforoushan *et al*. (2003) and Vernant *et al*. (2004) showed that the rate of shortening increases from 4 ± 2 mm a^{-1} in the NW to 9 ± 2 mm a^{-1} in the SE Zagros. In a separate work, Tatar *et al*. (2002) installed a GPS network to measure the shortening and strain rates in the central Zagros. They presented two campaigns of GPS measurements that indicate a shortening rate of about 10 mm a^{-1} in the central Zagros.

This paper specifically addresses the question of present crustal movement across and along the Zagros mountain belt. Previous studies on GPS results in Iran covered either a smaller area of the Zagros (Tatar *et al*. 2002) or the whole country (Nilforoushan *et al*. 2003; Vernant *et al*. 2004) but at much lower density than our network. We present the results of three campaigns of GPS measurements for the period February 1998 to June 2001 at 35 stations in and beside the Zagros (Fig. 1). The main objective of this study is to determine how the continuing convergence between Arabia and central Iran (Asia) is accommodated within the Zagros belt.

Geological setting

The late Cretaceous–early Miocene closure of Neo-Tethys between Arabia and Eurasia led to underthrusting of continental margin sediments along the Main Zagros Reverse Fault during the early stages of collision (Stöcklin 1974; Stoneley 1981) (Fig. 1). During the subsequent continental convergence, the Zagros deformation front migrated southwestward and has driven the

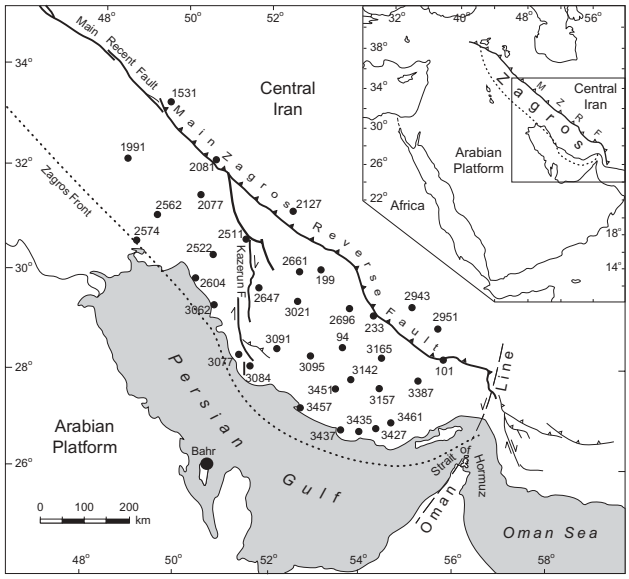

Fig. 1. Map of the Zagros region, SW Iran, showing GPS stations with identity number (●). Half-arrows show sense of motion along strike-slip faults. Bold lines with triangles on hanging wall show reverse faults.

foreland basin in front of it to its present position along the Persian Gulf and in Mesopotamia (Falcon 1974; Hessami *et al*. 2001*b*). The current plate margin (the Zagros deformation front) can be defined by seismogenic thrusts in the basement, which underlie folds in the sedimentary cover representing mainly thin-skinned shortening above the basement (Falcon 1974).

The Zagros is divided into two distinct along-strike blocks by the north–south-trending Kazerun Fault (Fig. 1). West of the Kazerun Fault, the Zagros Simply Folded Zone is a high-taper wedge (*c*. 2°) above a high-friction contact between the Phanerozoic cover and its Precambrian basement, whereas to the east the taper is lower (<1°) and pierced by diapirs of Hormuz salt that lubricate the sole of the wedge (Talbot & Alavi 1996). The Zagros has since been subdivided into other blocks bounded by north–south basement faults with or without basal detachments along the Hormuz salt (Bahroudi & Koyi 2003).

Most focal mechanism solutions of earthquakes in the Zagros region indicate the presence of active reverse faults in the uppermost part of the Arabian basement, beneath the Hormuz Salt Formation (Jackson & McKenzie 1984; Ni & Barazangi 1986). The active Mountain Front Fault is considered to be a major seismogenic reverse fault in the Zagros basement (Berberian 1995) (Fig. 2). NW of the Kazerun Fault, most moderate to large earthquakes occur near the Mountain Front Fault, whereas to the SE the same structure has lower seismic activity. Active basement thrusting SE of the Kazerun Fault occurs about 100 km behind the Mountain Front Fault.

GPS measurements and analysis

A GPS network consisting of 35 stations was installed in 1998 to study deformation in the Zagros Mountains (Fig. 1). Three campaigns of GPS measurement used dual-frequency GPS receivers in 1998, 1999 and 2001. The 1998 campaign used four System 200 Leica receivers with geodetic antenna during February and March. The 1999 and 2001 campaigns used six Trimble 4000 SSI GPS receivers with choke ring antennas in December and May, respectively. The limited number of receivers did not allow the complete network to be measured in one session. Instead, four or six GPS receivers were used simultaneously to measure the stations in different 8 h sessions day by day. However, because each station was remeasured in different sessions, the minimum time of observation for each station was 24 h.

The GPS data were processed using GAMIT, version 10.05 (King & Bock 2001) and GLOBK, version 10.0 (Herring 2001) software. GAMIT's automatic data cleaning routines were used to flag or correct cycle slips and remove poorly fitting data prior to the least-squares solution of double difference equations. The cleaned data were then processed in a GAMIT least-squares solution with full station coordinate and satellite orbit estimation using the ionosphere-free linear combination. We included observations of 4–6 IGS (International GNSS Service) stations with their positions and velocities in ITRF2000 (Altamimi *et al*. 2002) to tie our local data to the global reference frame (ITRF2000).

We solved for station coordinates, satellite state vectors, six tropospheric zenith delay parameters per site and day, and phase ambiguities using doubly differenced GPS phase measurements. We also used IGS final orbits, IERS (International Earth Rotation Service) Earth rotation parameters (EOP), and, following the tables recommended by the IGS (Rothacher & Mader 1996), we applied azimuth- and elevation-dependent antenna phase centre models. Finally, fixing phase ambiguities to integer values was attempted where possible.

The loosely constrained estimates of station coordinates and orbits and their covariances from each day were used as quasi-observations in a Kalman filter to estimate a consistent set of coordinates and velocities. We combined our daily solutions with SOPAC (Scripps Orbit and Permanent Array Center) daily solutions (available at http://lox.ucsd.edu). We also applied generalized constraints (Dong *et al*. 1998) while estimating a six-parameter transformation (six components of the rate of change of translation and rotation).

To define a reference frame for our velocity estimates, we followed the strategy described by McClusky *et al*. (2000) and defined a Eurasian frame by minimizing the horizontal velocities of 16 IGS stations located in the stable Eurasian plate (Table 1). However, for our final solution, the monthly averages of global solutions were used from the beginning of 1998 to the end of our survey in 2001. The root-mean-square (r.m.s.) departure of the velocities of the 16 IGS stations was less than 1 mm a^{-1} after transformation.

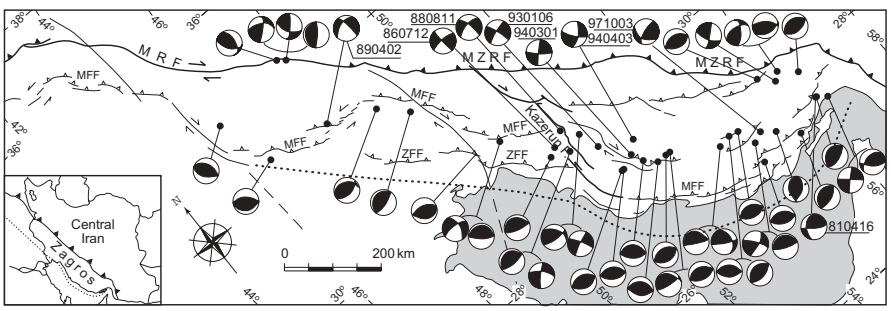

Fig. 2. Focal mechanism solutions of some of the Zagros earthquakes with their epicentral locations. The focal mechanisms are from Dziewonski *et al*. (1981, Harvard Centroid Moment Tensor solutions, which are marked with the date, y.m.d., on the focal sphere) and Chandra (1984). The NE limit of the belt is marked by the Main Zagros Reverse Fault (MZRF) and its NW extension, the Main Recent Fault (MRF). MFF, Mountain Front Fault; ZFF, Zagros foredeep fault.

Table 1. *GPS site velocities and 1σ uncertainties with respect to the Eurasian-fixed and Arabian-fixed reference frames*

Site	Long. (°E)	Lat. (°N)	Eurasia-fixed					Arabia-fixed	
			E vel.	N vel.	E σ*	N σ*	ρEN†	V_e	V_n
94	53.631	28.624	−0.83	15.26	1.14	0.8	−0.053	−3.58	−7.35
101	55.895	28.315	3.63	14.07	1.6	1.26	0.134	0.23	−9.84
1531	49.789	33.307	−1.57	15.94	2.02	1.16	0.189	−0.29	−4.38
199	53.146	30.087	−2.64	13.8	1.04	0.7	−0.088	−4.28	−8.52
1991	48.818	32.233	−2.94	15.97	1.26	0.86	0.049	−2.25	−3.76
2077	50.451	31.538	−6.07	17.49	1.1	0.72	0.043	−6.18	−3.23
2081	50.799	32.199	−2.79	13.4	1.32	0.88	0.026	−2.5	−7.53
2127	52.521	31.216	−0.82	13.14	1.26	0.82	−0.062	−1.56	−8.82
233	54.316	29.239	1.5	12.56	1.48	0.86	−0.047	−0.96	−10.4
2511	51.442	30.715	−4.49	14.09	1.04	0.64	−0.042	−5.37	−7.23
2522	50.734	30.386	−0.72	16.9	1.28	1.04	−0.028	−1.7	−3.99
2562	49.476	31.157	−3.57	18.01	1	0.6	0.059	−3.77	−2.12
2574	49.011	30.664	−2.76	16.25	1.1	0.8	0.012	−3.23	−3.6
2604	50.33	29.93	−0.55	18.28	1.42	0.92	−0.02	−1.78	−2.37
2647	51.755	29.732	−3.69	18.34	1.26	0.72	−0.081	−5.32	−3.16
2661	52.664	30.058	0.62	12.99	1.08	0.8	−0.046	−0.95	−9.05
2696	53.783	29.331	0.81	11.58	1.24	0.88	−0.079	−1.48	−11.1
2943	55.19	29.336	0.26	9.99	1.42	1.2	0.06	−2.3	−13.5
2951	55.78	28.936	2.19	11.59	1.18	0.86	−0.022	−0.76	−12.3
3021	52.639	29.477	2.93	12.68	1	0.7	−0.047	0.96	−9.35
3062	50.755	29.402	−1.2	17.41	1.04	0.72	0.004	−2.88	−3.49
3077	51.304	28.431	−1.82	18.17	1.58	0.96	0.056	−4.28	−3.06
3084	51.551	28.191	0.69	20.31	1.42	1.08	−0.054	−1.98	−1.07
3091	52.164	28.542	2.83	19.58	2.08	1.24	−0.047	0.3	−2.17
3095	52.903	28.392	0.32	15.42	0.98	0.72	0.011	−2.45	−6.76
3142	53.805	27.918	0.85	13.52	0.84	0.64	−0.01	−2.42	−9.19
3157	54.463	27.751	2.73	14.71	0.98	0.78	−0.018	−0.77	−8.38
3165	54.503	28.342	2.21	16.1	1.16	0.94	0.08	−0.9	−7.01
3387	55.32	27.939	0.8	14.93	0.96	0.76	0.02	−2.74	−8.65
3427	54.381	26.937	3.43	20.59	0.78	0.62	0.001	−0.62	−2.45
3435	54.004	26.883	4.35	20.4	1.16	0.98	0.051	0.34	−2.42
3437	53.596	26.92	5.26	17.31	1	0.78	0.024	1.34	−5.28
3451	53.476	27.736	2.95	17.12	0.92	0.7	−0.012	−0.38	−5.4
3457	52.685	27.36	0.73	17.41	1.58	1.02	−0.105	−2.72	−4.64
3461	54.723	27.06	4.79	21.56	0.84	0.7	0	0.77	−1.68
BAHR	50.608	26.209	3.1	18.65	0.46	0.34	−0.053	−0.8	−2.17
IGS sites used to define Eurasian fixed reference frame									
BOR1	17.073	52.277	0.88	0.22	0.16	0.15	0.034		
BRUS	4.359	50.798	−0.64	−1.25	0.13	0.12	−0.034		
GRAS	6.921	43.755	−0.15	0.44	0.12	0.11	0.017		
GRAZ	15.493	47.067	0.34	0.57	0.14	0.13	0.005		
IRKT	104.32	52.219	−0.49	−0.03	0.13	0.11	0.091		
JOZE	21.032	52.097	0.01	−0.13	0.18	0.17	−0.025		
KIT3	66.885	39.135	0.99	−0.44	0.13	0.09	−0.022		
KOSG	5.81	52.178	−0.26	0.42	0.09	0.09	−0.053		
POL2	74.694	42.68	0.93	3.18	0.15	0.1	−0.1		
WTZR	12.879	49.144	−0.31	0.08	0.11	0.09	−0.021		
ZECK	41.565	43.788	0.49	0.94	0.15	0.1	−0.033		
ARTU	58.56	56.43	−1.23	−0.39	0.68	0.47	−0.03		
ZIMM	7.465	46.877	0.98	0.57	0.16	0.14	−0.004		
ZWEN	36.759	55.699	0.3	−0.3	0.23	0.17	−0.002		
METS	24.395	60.217	−0.47	−0.54	0.15	0.13	0.068		
ONSA	11.926	57.395	−1.11	−0.04	0.1	0.1	0.046		

Station velocities and their uncertainties are given in mm a^{-1}. The Eurasian frame was determined by minimizing the horizontal velocity adjustments of the 16 stations given at the end of the table. *A priori* velocities for these stations were set to zero except for POL2 and KIT3 (*a priori* velocity of 2 mm a^{-1} north and 0.5 mm a^{-1} east).

*1σ uncertainties.

†Correlation coefficient between the east and north uncertainties. Arabian-fixed velocities were estimated using the Euler vector published by Vernant *et al*. 2004. However, the uncertainties are the same for Arabia-fixed velocities.

The formal errors are usually not considered as real uncertainties. Error analysis was performed in different steps. The position of each station was individually checked for possible systematic errors. The mean repeatabilities of baseline components average in the order of 1, 1.3 and 3 mm in north, east and height, respectively, for the three campaigns. The second and third campaign solutions show slightly better repeatability as a result of improvement of orbits in 1999 and 2001. In addition to random errors in the station position estimates, we added a random walk component equal to 2 mm a^{-1} (McClusky *et al*. 2000) to take into account the coloured noise and to deal with possible monument instability (Langbein & Johnson 1997). Figure 3 shows the detrended residual series for two sampled stations and indicates how well the long-

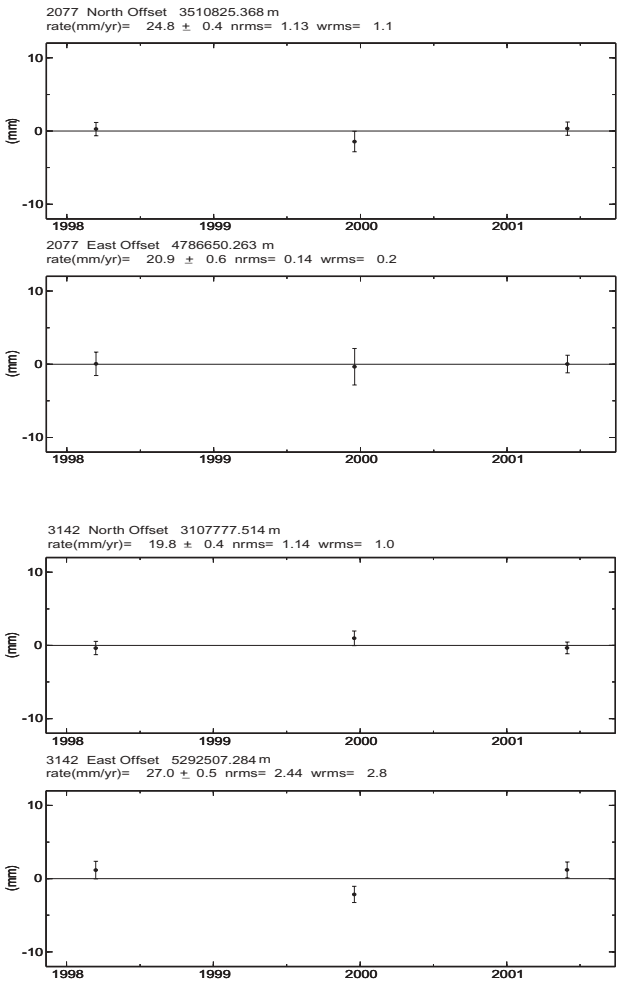

Fig. 3. Time series of geocentric position of stations 2077 and 3142 located in the west and east Zagros, respectively, after removing the best-fit straight line. Labels show estimated rate with respect to ITRF2000, its 1σ uncertainty, and the normalized (nrms, in mm) and weighted (wrms, in mm) root-mean-square scatters.

term repeatabilities of the three surveys are aligned. We found normalized and weighted r.m.s. scatters to be less than 3 mm for these surveys.

Results

Figure 4 shows the velocity vectors for the Zagros GPS stations averaged over the 40 months of three campaigns in a Eurasia-fixed reference frame (see also Table 1). Figure 4 discloses two areas of movement within the Zagros belt. East of the Kazerun Fault, stations moved between 13 and 22 mm a^{-1} towards N 7 ± 5°E. West of the Kazerun Fault, stations moved towards N 12 ± 8°W at 14–19 mm a^{-1}.

To emphasize internal Zagros deformation, we also estimated velocities in an Arabia-fixed reference frame (Fig. 5) using the Arabia–Eurasia Euler vector (27.9 ± 0.5°N, 19.5 ± 1.4°E, 1.41 ± 0.1° Ma^{-1}) calculated by Vernant *et al.* (2004). East of the Kazerun Fault the velocity vectors move SSW (±10° from S 10°W) at rates that range from 2 to 13 mm a^{-1} (Fig. 5 and Table 1). West of the Kazerun Fault, stations moved towards S 35 ± 10°W at 3–9 mm a^{-1} (Fig. 5 and Table 1). The oblique motion of the NW Zagros requires right-lateral movement of

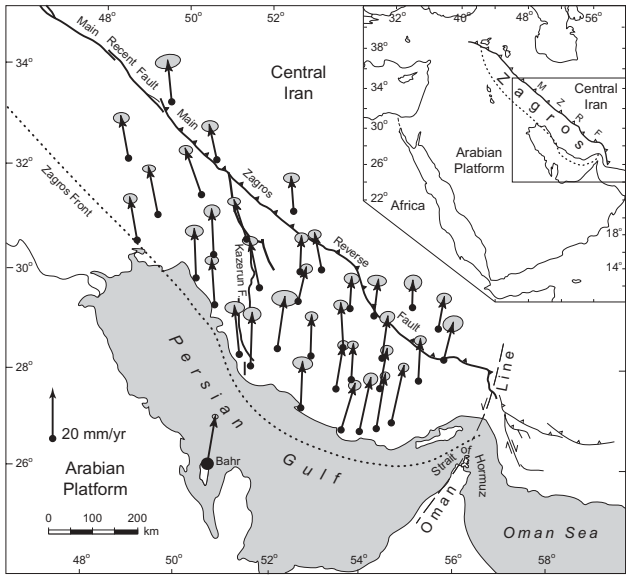

Fig. 4. GPS horizontal velocities and their 95% confidence ellipses in a Eurasia-fixed reference frame for the period 1998–2001. Formal errors are scaled by a factor of two calculated from the ratio χ^2/degree of freedom of velocity solution.

about 3–4 mm a^{-1} along the northwestern segment of the Main Zagros Reverse Fault (i.e. the southeastern continuation of the Main Recent Fault; Figs 4 and 5). West of the Kazerun Fault most of the shortening indicated by the GPS velocities seems to occur along the Mountain Front Fault as well as along the Zagros front.

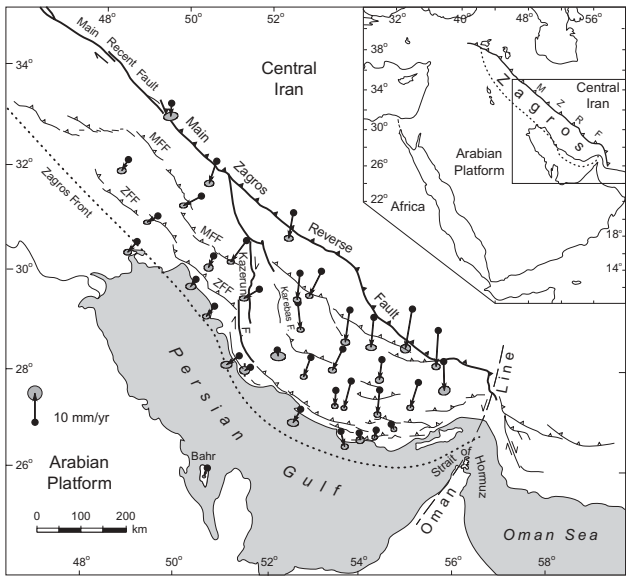

Fig. 5. GPS horizontal velocities and their 95% confidence ellipses in the Arabia-fixed reference frame for the period 1998–2001. The velocities were estimated using the Euler vector calculated by Vernant *et al.* (2004) to show the present-day shortening in the Zagros (i.e. the northern margin of Arabia). The very small velocities (at the level of our 3 mm a^{-1} error estimates) of the stations close to the Persian Gulf suggest that shortening diminishes southwestwards in the Zagros fold–thrust belt.

Most of the stations (3427, 3435, 3437, 3457 and 3084 in Figs 1 and 5) just behind the deformation front moved more slowly than those further behind (i.e. 3095, 3142 and 3157), indicating that some shortening occurs by folding or faulting within the SE Zagros belt as well as along the Zagros front (Fig. 5). This shortening occurs along the zone where major earthquakes are indicated in the SE Zagros (Fig. 2). Shortening is slower both in front of and behind this seismic zone. However, two stations (2943 and 2951) behind the Main Zagros Reverse Fault moved about 3–4 mm a^{-1} faster than the average rate (9 mm a^{-1}) for the stations (101, 233, 3165 and 3387 in Figs 1 and 5) in front of the Main Zagros Reverse Fault. The 3–4 mm a^{-1} differences suggest that the southeastern segment of the old suture zone (Main Zagros Reverse Fault) is still active.

The 2–3 mm a^{-1} difference between the velocities of BAHR on stable Arabia and stations 2574, 3062, 3077, and 3457 (Figs 1 and 5) is probably accommodated along the Zagros front and implies that any shortening is negligible in that sector.

Velocity vectors in Figure 5 imply that the Kazerun Fault and other strike-slip faults east of it (such as the Karebas Fault) are right-lateral with oblique normal slip at up to 4–5 mm a^{-1}, in agreement with focal mechanism solutions of earthquakes along the Kazerun and Karebas fault zones (Talebian & Jackson 2004).

Discussion

The dense velocity field obtained from three campaigns of GPS measurements along the Zagros Mountains shows clearly for the first time the change in character across the Kazerun Fault. East of the Kazerun Fault, the velocity vectors have roughly a north–south direction, and, on average, are nearly perpendicular to the arcuate trend of the geological structures. However, west of the Kazerun Fault the velocity vectors are oblique to the linear trend of the mountain belt (Fig. 4). The general NW to SE increase in velocity along the entire Zagros belt can be attributed to the anticlockwise rotation of Arabia relative to Eurasia around small circles concentric about the rotation pole at 27.9°N, 19.5°E (Fig. 5 and Table 1). The component of deformation that results from the change in direction of the velocity vectors across the Kazerun and Karebas faults involves extension parallel to the strike of the belt (Fig. 4). This extension, at a rate of up to 4 mm a^{-1}, is due largely to the Kazerun and Karebas strike-slip faults rotating about vertical axes. Other studies have also suggested that along-strike extension east of the Kazerun Fault is an important element in the Zagros tectonics (Baker *et al*. 1993; Hessami *et al*. 2001*a*; Talebian & Jackson 2004). The extension parallel to the strike of the belt implies that the deformation caused by relative motion between Arabia and central Iran is not accommodated by simple across-strike shortening and thickening.

The velocity field in Figure 5 correlates well with the seismicity (see Fig. 2). That is, west of the Kazerun Fault the largest shortening indicated by the GPS velocities seems to occur along the Mountain Front Fault, whereas SE of the Kazerun Fault most of the shortening occurs about 100 km north of the Mountain Front Fault. In addition, there is clear shortening across the southeastern segments of the Main Zagros Reverse Fault. These zones correspond closely to the areas where the seismicity is concentrated. Comparison of velocities deduced from GPS measurements in the SE Zagros with shortening rates of 1–2 mm a^{-1} calculated from summing seismic moments (Shoja-Taheri & Niazi 1981; Jackson & McKenzie 1988) implies that as little as 15–20% of the total shortening (9 ± 3 mm a^{-1}) across the Zagros is accommodated seismically on basement faults. This may suggest that most of the continuing deformation within the SE Zagros is accommodated by aseismic extension parallel to the strike as well as by aseismic shortening perpendicular to the belt. However, a second explanation for the discrepant 7–8 mm a^{-1} is that it is taken up by elastic strain currently accumulating on both sides of the faults during a continuing inter-seismic period.

Comparison of our GPS velocities with results for some of the stations in the network used by Tatar *et al*. (2002) shows large discrepancies of about 6 mm a^{-1} in velocity vectors. We attribute these differences to our time spans being longer (40 v. 24 months), over more campaigns (three versus two campaigns) and, to some extent, to our slightly different set of fixed IGS stations. In fact, Tatar *et al*. (2002) selected one non-fixed Eurasian IGS station (their MATE IGS station is moving 1.67 mm a^{-1} eastward and 4.31 mm a^{-1} northward (see McClusky *et al*. 2003)) for realization of their reference frame. However, there are small mean differences of about 2 mm a^{-1} in both north and east velocities between our velocity vectors and a few of the stations in the network used by Vernant *et al*. (2004).

Conclusion

GPS measurements and analyses of the 1998, 1999 and 2001 campaigns indicate that the current rate of shortening across the SE Zagros is about 9 ± 3 mm a^{-1}, whereas in the NW Zagros it is about 5 ± 3 mm a^{-1}. This is consistent with the previous results published by Vernant *et al*. (2004). The GPS velocities also indicate that shortening is not distributed homogeneously either along or across the belt. In the NW Zagros (west of the Kazerun Fault) shortening is accommodated mainly along the Mountain Front Fault, where most of the major earthquakes occur, and along the Zagros front. East of the Kazerun Fault, however, fastest shortening seems to occur along a zone of active thrusting within the SE Zagros and along the old suture zone (Main Zagros Reverse Fault), both areas where seismicity is concentrated. The along-strike extension of the Zagros belt across the Kazerun and Karebas faults implies that the deformation in this mountain belt is not accommodated by simple across-strike shortening and thickening.

We thank H. G. Scherneck, J. A. Jackson, R. W. King, H. A. Koyi and L. Sjöberg for comments and for suggesting improvements to earlier drafts of this manuscript. We are also indebted to M. Pan, M. Ghafori-Ashtiany, F. Tavakoli, H. R. Nankali, E. Shabanian and H. Tabassi for help. We wish to thank R. Reilinger and C. Vigny for their constructive reviews, which substantially improved the original manuscript. This research was funded by the National Cartographic Center (NCC), Tehran, and International Institute of Earthquake Engineering and Seismology (IIEES), Tehran. We are grateful to the many individuals at NCC who contributed, in one way or another, to the acquisition of the GPS data. K.H. and F.N. acknowledge PhD grants from Uppsala University.

References

Altamimi, Z., Sillard, P. & Boucher, C. 2002. ITRF2000: a new release of the International Terrestrial Reference Frame for earth science applications. *Journal of Geophysical Research*, **107**, doi: 10.1029/2001JB000561.

Bahroudi, A. & Koyi, H.A. 2003. The effect of spatial distribution of Hormuz salt on deformation style in the Zagros fold and thrust belt: an analogue modelling approach. *Journal of the Geological Society, London*, **160**, 719–733.

Baker, C., Jackson, J. & Priestley, K. 1993. Earthquakes on the Kazerun Line in the Zagros mountains of Iran: strike-slip faulting within a fold-and-thrust belt. *Geophysical Journal International*, **115**, 41–61.

Berberian, M. 1995. Master 'blind' thrust faults hidden under the Zagros folds: active basement tectonics and surface morphotectonics. *Tectonophysics*, **241**, 193–224.

Chandra, U. 1984. Focal mechanism solution for earthquakes in Iran. *Physics of the Earth and Planetary Interiors*, **34**, 9–16.

DeMets, C., Gordon, R.G., Argus, D.F. & Stein, S. 1990. Current plate motions. *Geophysical Journal International*, **101**, 425–478.

Dong, D., Herring, T.A. & King, R.W. 1998. Estimating regional deformation from a combination of space and terrestrial geodetic data. *Journal of Geodesy*, **72**, 200–211.

Dziewonski, A.M., Chow, T.A. & Wookhouse, J.H. 1981. Determination of earthquake source parameters from waveform data for studies of global and regional seismicily. *Journal of Geophysical Research*, **86**, 2825–2852.

Falcon, N.L. 1974. Southern Iran: Zagros Mountains. *In:* Spencer, A. (ed.) *Mesozoic–Cenozoic Orogenic Belts*. Geological Society, London, Special Publications, **4**, 199–211.

Herring, T.A. 2001. *Documentation for the GLOBK software version 9.5*. Massachusetts Institute of Technology, Cambridge, MA.

Hessami, K., Koyi, H.A. & Talbot, C.J. 2001a. The significance of strike-slip faulting in the basement of the Zagros fold and thrust belt. *Journal of Petroleum Geology*, **24**, 5–28.

Hessami, K., Koyi, H.A., Talbot, C.J., Tabasi, H. & Shabanian, E. 2001b. Progressive unconformities within an evolving foreland fold–thrust belt, Zagros Mountains. *Journal of the Geological Society, London*, **158**, 969–981.

Jackson, J. & McKenzie, D.P. 1988. The relationship between plate motions and seismic moment tensors, and the rates of active deformation in the Mediterranean and Middle East. *Geophysical Journal*, **93**, 45–73.

Jackson, J. & McKenzie, D.P. 1984. Active tectonics of Alpine–Himalayan belt between western Turkey and Pakistan. *Geophysical Journal of the Royal Astronomical Society*, **77**, 185–264.

King, R.W. & Bock, Y. 2001. *Documentation for the GAMIT GPS software analysis version 10.05*. Massachusetts Institute of Technology, Cambridge, MA.

Langbein, J. & Johnson, H. 1997. Correlated errors in geodetic time series: implications for time-dependent deformation. *Journal of Geophysical Research*, **102**, 591–603.

Lees, G.M. & Falcon, N.L. 1952. The geographical history of the Mesopotamian Plains. *Geographical Journal*, **118**, 24–39.

Le Pichon, X.L. 1968. Sea floor spreading and continental drift. *Journal of Geophysical Research*, **73**, 3661–3697.

McClusky, S., Balassanian, S. & Barka, A. *et al.* 2000. Global Positioning System constraints on plate kinematics and dynamics in the eastern Mediterranean and Caucasus. *Journal of Geophysical Research*, **105**, 5695–5719.

McClusky, S., Reilinger, R., Mahmoud, S., Ben Sari, D. & Tealeb, A. 2003. GPS constraints on Africa (Nubia) and Arabia plate motions. *Geophysical Journal International*, **155**, 126–138.

McKenzie, D.P. 1972. Active tectonics of the Mediterranean region. *Geophysical Journal of the Royal Astronomical Society*, **30**, 109–185.

Ni, J. & Barazangi, M. 1986. Seismotectonics of the Zagros continental collision zone and a comparison with the Himalayas. *Journal of Geophysical Research*, **91**, 8205–8218.

Nilforoushan, F., Vernant, P. & Masson, F. *et al.* 2003. GPS network monitors the Arabia–Eurasia collision deformation in Iran. *Journal of Geodesy*, **77**, 411–422.

Rothacher, M. & Mader, G. 1996. *Combination of antenna phase center offsets and variations: antenna calibration set IGS01*. IGS Central Bureau–University of Berne, Berne.

Shoja-Taheri, J. & Niazi, M. 1981. Seismicity of the Iranian Plateau and bordering regions. *Bulletin of the Seismological Society of America*, **71**, 477–489.

Stöcklin, J. 1974. Possible ancient continental margins in Iran. *In:* Burk, C.A. & Drake, C.L. (eds) *The Geology of Continental Margins*. Springer, New York, 873–887.

Stoneley, R. 1981. The geology of the Kuh-e Dalneshin area of southern Iran and its bearing on the evolution of southern Tethys. *Journal of the Geological Society, London*, **138**, 509–526.

Talbot, C.J. & Alavi, M. 1996. The past of a future syntaxis across the Zagros. *In:* Alsop, G.I., Blundell, D.J. & Davison, I. (eds) *Salt Tectonics*. Geological Society, London, Special Publications, **100**, 89–109.

Talebian, M. & Jackson, J. 2004. A reappraisal of earthquake focal mechanisms and active shortening in the Zagros Mountains of Iran. *Geophysical Journal International*, **156**, 506–526.

Tatar, M., Hatzfeld, D., Martinod, J., Walpersdorf, A., Ghafori-Ashtiany, M. & Chéry, J. 2002. The present-day deformation of the central Zagros from GPS measurements. *Geophysical Research Letters*, **29**, 101029/2002/GL015427.

Vernant, P., Nilforoushan, F. & Hatzfeld, D. *et al.* 2004. Present-day crustal deformation and plate kinematics in Middle East constrained by GPS measurements in Iran and northern Oman. *Geophysical Journal International*, **157**, 381–398.

Vita-Finzi, C. 1979. Rates of Holocene folding in the coastal Zagros near Bandar Abbas, Iran. *Nature*, **278**, 632–634.

Received 21 February 2005; revised typescript accepted 30 May 2005.
Scientific editing by Ian Alsop